ANALELE UNIVERSITĂȚII
"EFTIMIE MURGU" REȘIȚA
ANUL XVII, NR. 1, 2010, ISSN 1453 - 7397

Stelian Mihalcea

A Kinematic Analysis of the Variable Valve Timing Mechanism with Three Elements and Continuous Valve Lift

An innovating solution for throttle-free load control for spark-ignition engines is Variable Valve Timing system (VVT System, or VVA - Variable Valve Actuation System). In this paper is presented an analytic method for kinematic analysis of the valve timing mechanism with three elements, which mainly includes the camshaft, the roller rocker finger and an intermediate rocker arm. This type of mechanism ensures a continuous valve lift (VVL System) between two extreme valve heights. It is also presented the numerical example for the variable valve lift mechanism's motion.

Keywords: *Variable Valve Lift, Mechanism, Kinematic analysis*

1. Introduction

For the traditional spark-ignition engines the timing configuration does not allow the best engine performance to be achieved for all regime and load. Infinitely variable inlet valve lift and timing is used to control engine load, reducing throttling losses and fuel consumption [8]. It also improves low-end torque and transient response.

Variable valve timing technology allows better engine performance by reducing fuel consumption and therefore low emissions [5], higher efficiency, highly precise responsiveness of the powertrain [7].

The key parameter for petrol engine combustion, and therefore efficiency, emissions and fuel consumption is the quantity and characteristics of the fresh air charge in the cylinders. In conventional petrol engines, the throttle-based air control wastes about 10% of the input energy in pumping the air [9]. VVT systems with continuous valve lift variation, usually combined with cam phasers, are designed to eliminate the classical throttle and it's inconvenient.

2. The proposed mechanism

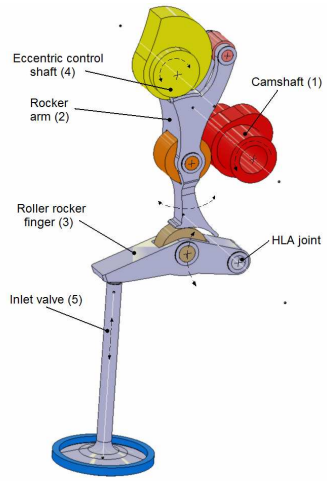

Figure 1. Design and functionality of the VVL mechanism

The mechanism is a mechanical, continuously VVL system, used for the first time on the spark-ignition engines by the German car manufacturer BMW. The main difference that sets this mechanism apart from a regular one is the presence of an additionally rocker arm between the camshaft and the standard roller cam follower. The motion is transmitted by the camshaft (1) to the roller rocker finger (3) via the rocker arm (2) which is equipped with a working curve. The rocker arm is in a direct and permanent support with the camshaft, the eccentric control shaft (4) and the roller rocker finger with the working curve. For each angle of the control shaft, there is a maximum and fixed intake valve (5) lift. Variation of the valve lift is achieved by modifying the eccentric shaft position.

3. Mechanism kinematic analysis
3.1. The rocker arm working curve

For the proposed mechanism, the kinematic schema is showed in figure 2; accordingly with the notations there are 4 sliding contact between the elements C_1, C_2, C_3, C_4. Also the camshaft and the roller rocker finger are articulated with the base (cylinder head) in O_1 and O_4. Therefore, the mechanism's mobility is unique, as it results from [3]:

$$M_3 = 3 \cdot n - 2 \cdot c_5 - c_4 = 3 \cdot 3 - 2 \cdot 2 - 4 = 1. \quad (1)$$

The eccentric control shaft has no influence on the mechanism's mobility because its position is stationary. The general coordinate system is O_0XY, the camshaft (1) local coordinate system is $O_1x_1y_1$ where O_1 is identically positioned with O_0, the rocker arm (2) local coordinate system is $O_2x_2y_2$ where point A is placed on the O_2y_2 axis, the roller rocker finger (3) local coordinate system is $O_3x_3y_3$ where point E is placed on the O_3x_3 axis.

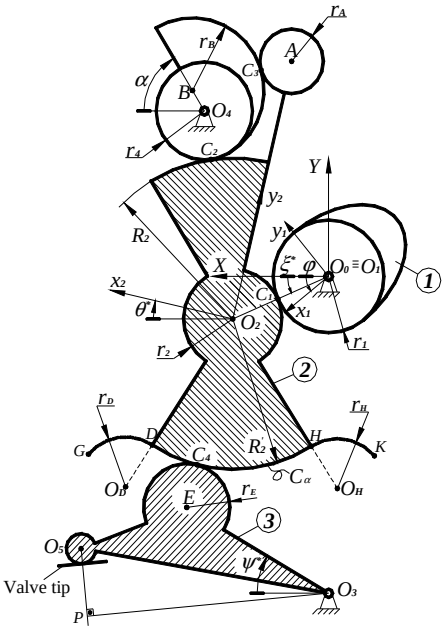

Figure 2. Mechanism's kinematic schema, and computing notations

When the eccentric shaft is turning (measured with the angle $\alpha \in [\alpha_{\min};\alpha_{\max}]$), the rocker arm (2) is turning around the point O_2, the contact C_4 with the roller rocker (3) describes a contact curve (working curve) C_α, which is actually the DH circle arch by $R_2^{'}$ radius; the point D matches the $\alpha_{\min}$ angle and point H to the $\alpha_{\max}$.

To ensure the permanent contact between elements (2) and (3) is necessary to extend the C_α curve with two circle arches DG, HK, and so results the contact curve (working curve) Γ (figure 2).

Some notations are used:

- $l_1 = O_2A,\ l_2 = O_4B,\ l_3 = O_3E,\ l_4 = O_3O_5,\ l_5 = O_3P$;
- $r_1,\ r_2,\ R_2,\ R_2^{'},\ r_4,\ r_A,\ r_B,\ r_E,\ r_D,\ r_H$, for the circles radii in figure 2;
- $\xi^*,\ \theta^*,\ \psi^*$, on the mechanism's reference position ($\varphi = \varphi^* = 0$), between $O_0O_2,\ O_2x_2,\ O_3E$, axis and O_0X axis; also are used some secondary angles $\xi_2,\ \xi_3,\ \xi_4$ to define the contact equations for $C_2,\ C_3$ and C_4 points (figure 3, 4, 5);
- $O_3(X_3, Y_3)$ and $O_4(X_4, Y_4)$ point coordinates in the main coordinates system O_0XY.

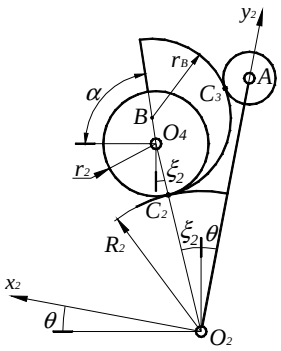

Figure 3. The C_2 contact point

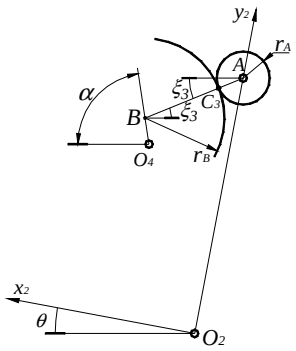

Figure 4. The C_3 contact point

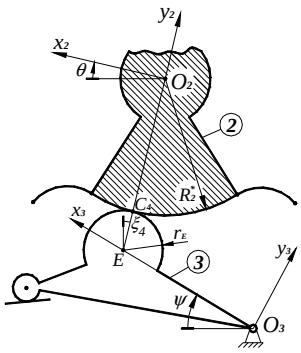

Figure 5. The C_4 contact point

The $\xi^*,\ \psi^*$ angles and the O_2 general coordinates $X_2^*,\ Y_2^*$ for the mechanism's reference position ($\varphi = \varphi^* = 0$), do not depend on the eccentric shaft setting angle α and therefore some consecutively elementary relations are obtained:

$$\xi^* = \arccos\frac{X_4^2 + Y_4^2 + (r_1 + r_2)^2 - (r_4 + R_2)^2}{2(r_1 + r_2)\sqrt{X_4^2 + Y_4^2}} - \arccos\frac{X_4}{\sqrt{X_4^2 + Y_4^2}}, \tag{2}$$

$$X_2^* = (r_1 + r_2)\cos\xi^*;\ \ Y_2^* = -(r_1 + r_2)\sin\xi^*, \tag{3}$$

$$\psi^* = \operatorname{arctg}\frac{Y_2^* - Y_3}{X_2^* - X_3} - \arccos\frac{l_3^2 + l_{O_2O_3}^2 - (R_2^{'} + r_E)^2}{2l_3 l_{O_2O_3}}; \tag{4}$$

$$l_{O_2O_3} = \sqrt{(X_3 - X_2^*)^2 + (Y_3 - Y_2^*)^2},$$

$$X_E^* = X_3 + l_3 \cos\psi^*;\ Y_E^* = Y_3 + l_3 \sin\psi^*. \tag{5}$$

The θ^* angle varies with the variation of command angle α. The α angle will be named η when the parametric equation of C_α curve will be developed. Angle θ^* results form following consecutively relations:

$$X_B^* = X_4 + l_2 \cos\alpha;\ Y_B^* = Y_4 + l_2 \sin\alpha, \tag{6}$$

$$\theta^* = \arccos\frac{X_B^* - X_2^*}{l_{O_2B}} + \arccos\frac{l_1^2 + l_{O_2B}^2 - (r_A + r_B)^2}{2 l_1 l_{O_2B}} - \frac{\pi}{2},$$
$$l_{O_2B} = \sqrt{(X_B^* - X_2^*)^2 + (Y_B^* - Y_2^*)^2}. \tag{7}$$

Once the θ^* angle and O_2 general position are known, the A point general position results:

$$X_A^* = X_2^* - l_1 \sin\theta^*;\ Y_A^* = Y_2^* + l_1 \cos\theta^*. \tag{8}$$

The ξ_1 angle (figure 6), which define the C_1 contact point position in $O_2x_2y_2$ coordinate system, results from:

$$\xi_1^* = \xi^* + \theta^*. \tag{9}$$

The ξ_2 angle (figure 3), which define the C_2 contact point position in $O_2x_2y_2$ coordinate system, results from:

$$\xi_2^* = arctg\frac{X_4 - X_2^*}{Y_4 - Y_2^*}. \tag{10}$$

In the same way, the ξ_3 angle is defined (figure 4):

$$\xi_3^* = arctg\frac{Y_A - Y_B^*}{X_A - X_B^*}, \tag{11}$$

respectively the ξ_4 angle (figure 5):

$$\xi_4^* = arctg\frac{X_E^* - X_2^*}{Y_E^* - Y_2^*}. \tag{12}$$

Considering that the α angle is set on the extreme values $\alpha_{\min}$, $\alpha_{\max}$, for the θ^* angle results the extreme values $\theta_{\min}^*$, $\theta_{\max}^*$, and using the following notations

$$\theta_0 = \arccos\frac{X_3 \cos\psi^* + Y_3 - X_2^*}{R_2^{'} + r_E}, \tag{13}$$

$$\eta = \theta^* + \theta_0,\ \eta_{\min} = \theta_{\min}^* + \theta_0,\ \eta_{\max} = \theta_{\max}^* + \theta_0, \tag{14}$$

the parametrically equations in $O_2x_2y_2$ coordinates system for C_α curve (DH circle arch) are obtained:

$$x_{C_\alpha} = R_2^{'}\cos\eta;\ \ y_{C_\alpha} = -R_2^{'}\sin\eta, \tag{15}$$

where $\eta_{\min} \le \eta \le \eta_{\max}$.

If Γ curve is obtained by connecting in points D, H circles arches with r_D, r_H radius and if (x_D, y_D), (x_H, y_H) are the x_{C_α}, y_{C_α} coordinates values for the extreme angles $\eta_{\min}$, $\eta_{\max}$, the parametrically representation of the Γ curve in the local coordinates system $O_2x_2y_2$ is obtained

$$\begin{aligned} x_\Gamma &= \begin{cases} x_D + r_D\left[\cos\eta_{\min} - \cos(2\eta_{\min} - \eta)\right], & \text{if } \eta < \eta_{\min} \\ R_2^{'}\cos\eta, & \text{if } \eta_{\min} \le \eta \le \eta_{\max} \\ x_H + r_H\left[\cos\eta_{\max} - \cos(2\eta_{\max} - \eta)\right], & \text{if } \eta > \eta_{\max} \end{cases} \\ y_\Gamma &= \begin{cases} y_D - r_D\left[\sin\eta_{\min} - \sin(2\eta_{\min} - \eta)\right], & \text{if } \eta < \eta_{\min} \\ -R_2^{'}\sin\eta, & \text{if } \eta_{\min} \le \eta \le \eta_{\max} \\ y_H - r_H\left[\sin\eta_{\max} - \sin(2\eta_{\max} - \eta)\right], & \text{if } \eta > \eta_{\max} \end{cases} \end{aligned} \tag{16}$$

where:

$$x_D = r_D\cos\eta_{\min};\ \ y_D = r_D\sin\eta_{\min}, \tag{17}$$

$$x_H = r_H\cos\eta_{\max};\ \ y_H = r_H\sin\eta_{\max}. \tag{18}$$

3.2. Contact and tangency equations. Intake valve lift law

Considering that the cam parametric equations in the $O_1x_1y_1$ coordinates system are

$$x_1 = x_1(\xi);\ \ y_1 = y_1(\xi), \tag{19}$$

and the cam rotation angle with initial position is φ, then using the O_2 center circle parametric equations in $O_2x_2y_2$ and r_2 radius

$$x_2 = -r_2\cos\xi_1;\ \ y_2 = r_2\sin\xi_1, \tag{20}$$

the tangency and contact equations in point C_1 are obtained (figure 6):

$$f_1 = x_{1p}\cos(\varphi - \beta + \xi_1 - \theta) - y_{1p}\sin(\varphi - \beta + \xi_1 - \theta) = 0, \tag{21}$$

$$f_2 = x_1\cos(\varphi - \beta) - y_1\sin(\varphi - \beta) + r_2\cos(\xi_1 - \theta) - X_2 = 0, \tag{22}$$

$$f_3 = x_1\sin(\varphi - \beta) + y_1\cos(\varphi - \beta) - r_2\sin(\xi_1 - \theta) - Y_2 = 0, \tag{23}$$

where x_{1p} and y_{1p} are the x_1 and y_1 derivates with cam rotation angle φ, β is the angle which defines the cam position in its coordinates system, X_2 and Y_2 are the O_2 point coordinates in the general system O_0XY.

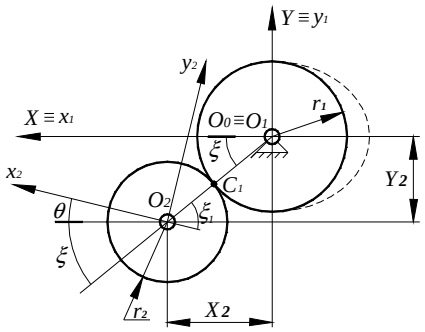

Figure 6. The C_1 contact point on the base cam circle

Knowing the ξ_2 angle between O_2O_4 and O_0Y axis, for the tangency contact point C_2 the following equations are obtained:

$$f_4 = X_2 + (R_2 + r_4)\sin\xi_2 - X_4 = 0, \tag{24}$$

$$f_5 = Y_2 + (R_2 + r_4)\cos\xi_2 - Y_4 = 0. \tag{25}$$

In the same way, knowing the ξ_3 angle between AB segment and O_0X axis, for the contact and tangency point C_3 the following equations are obtained:

$$f_6 = X_2 - l_1\sin\theta + (r_A + r_B)\cos\xi_3 - X_4 - l_2\cos\alpha = 0, \tag{26}$$

$$f_7 = Y_2 + l_1\cos\theta - (r_A + r_B)\sin\xi_3 - Y_4 - l_2\sin\alpha = 0. \tag{27}$$

For the contact and tangency in C_4 point, using the ξ_4 angle between EC_4 segment and O_0Y axis and knowing the (16) equations, results:

$$f_8 = X_2 + x_\Gamma\cos\theta - y_\Gamma\sin\theta - l_3\cos\psi + r_E\sin\xi_4 - X_3 = 0, \tag{28}$$

$$f_9 = Y_2 + x_\Gamma\sin\theta + y_\Gamma\cos\theta - l_3\sin\psi - r_E\cos\xi_4 - Y_3 = 0, \tag{29}$$

$$f_{10} = x_{\Gamma p}\sin(\xi_4 - \theta) - y_{\Gamma p}\cos(\xi_4 - \theta) = 0. \tag{30}$$

where

$$\begin{aligned} &x_{\Gamma p} = -r_D\sin(2\eta_{\min} - \eta);\ y_{\Gamma p} = -r_D\cos(2\eta_{\min} - \eta), && \text{if } \eta < \eta_{\min} \\ &x_{\Gamma p} = -R_2^*\sin\eta;\ y_{\Gamma p} = -R_2^*\cos\eta, && \text{if } \eta_{\min} \le \eta \le \eta_{\max} \\ &x_{\Gamma p} = -r_H\sin(2\eta_{\max} - \eta);\ y_{\Gamma p} = -r_H\cos(2\eta_{\max} - \eta), && \text{if } \eta > \eta_{\max} \end{aligned} \tag{31}$$

Equations $f_i = 0,\ i = 1, 2, ..., 10,$ form a system from where $\xi,\ \xi_1,\ \xi_2,\ \xi_3,\ \xi_4,\ X_2,\ Y_2,\ \theta,\ \psi,\ \eta,$ parameters are determined for $\varphi = 1 \div 360°$. The equations system is easily solved using the numerical computing method Newton-Raphson, in which the initial value are $\xi^*,\ \xi_1^*,\ \xi_2^*,\ \xi_3^*,\ \xi_4^*,\ X_2^*,\ Y_2^*,\ \theta^*,\ \psi^*,\ \eta$. Using the following notation

$$\gamma = \arccos\frac{l_6}{l_5}, \tag{32}$$

results the valve lift law

$$s(\varphi) = l_6\left[\sin\gamma - \sin\left(\gamma + \psi - \psi^*\right)\right]. \tag{33}$$

4. Numerical example

The approximate dimension used to validate the computational model are following: $\varphi = 0 \div 360°$, $\alpha = 0 \div 150°$, $\beta = 0°$, $r_1 = 12\,\text{mm}$, $O_1\left(X_{O_1}; Y_{O_1}\right) = (0; 0)\,\text{mm}$, $O_3\left(X_{O_3}; Y_{O_3}\right) = (-10; -43)\,\text{mm}$, $O_4\left(X_{O_4}; Y_{O_4}\right) = (25; 40)\,\text{mm}$, $r_4 = 10\,\text{mm}$, $r_B = 14\,\text{mm}$, $r_A = 5\,\text{mm}$, $r_2 = 7\,\text{mm}$, $R_2 = 31\,\text{mm}$, $R_2^{'} = 28\,\text{mm}$, $l_1 = 48\,\text{mm}$, $l_2 = 4\,\text{mm}$, $l_3 = 35\,\text{mm}$, $l_4 = 55\,\text{mm}$, $l_5 = 54{,}929\,\text{mm}$, $r_D = 10\,\text{mm}$, $r_H = 15\,\text{mm}$, $< (EO_3O_5) = 15°$.

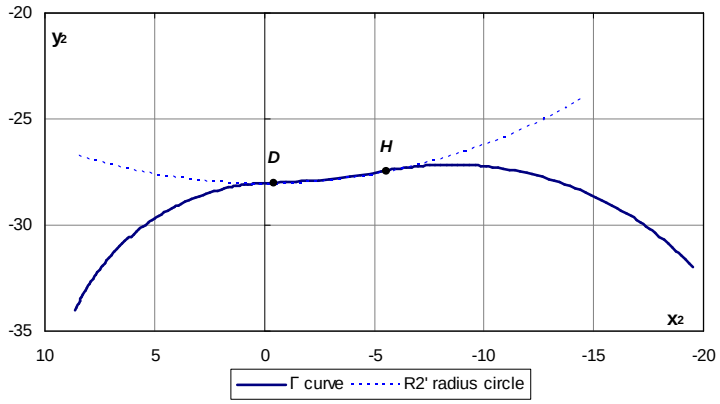

Figure 7. The Γ curve allure in $O_2x_2y_2$ coordinate system

The final mechanism dimensions will be established after the mechanism optimization procedure.

Using (2), (9), (10), (11), (12), (3), (7), (4), (14), and $\alpha=[\alpha_{\min};\alpha_{\max}]$, $\alpha_{\min}=0°$, $\alpha_{\max}=150°$, the results are stored in table 1. Also, using (13) results $\theta_0=81.583°$ and $\eta_{\min}=90.846°$ respectively, $\eta_{\min}=101.405°$. The curve Γ allure results from (16) and its design is presented in figure 7. In figure 8 are designed the reference positions for $\alpha=0,90,150°$, where O_1, O_3, O_4 represents the camshaft, roller rocker and eccentric shaft joints.

Table 1.

$\alpha[°]$	$\xi^*[°]$	$\xi_1^*[°]$	$\xi_2^*[°]$	$\xi_3^*[°]$	$\xi_4^*[°]$	$X_2^*[\text{mm}]$	$Y_2^*[\text{mm}]$	$\theta^*[°]$	$\psi^*[°]$	$\eta[°]$
0	1.681	10.945	8.427	21.025	8.417	18.992	-0.557	9.264	12.910	90.846
15	1.681	11.585	8.427	17.433	8.417	18.992	-0.557	9.903	12.910	91.486
30	1.681	12.443	8.427	14.006	8.417	18.992	-0.557	10.762	12.910	92.344
45	1.681	13.485	8.427	10.919	8.417	18.992	-0.557	11.804	12.910	93.387
60	1.681	14.674	8.427	8.321	8.417	18.992	-0.557	12.993	12.910	94.575
75	1.681	15.962	8.427	6.332	8.417	18.992	-0.557	14.281	12.910	95.864
90	1.681	17.293	8.427	5.047	8.417	18.992	-0.557	15.612	12.910	97.195
105	1.681	18.598	8.427	4.533	8.417	18.992	-0.557	16.917	12.910	98.500
120	1.681	19.796	8.427	4.829	8.417	18.992	-0.557	18.115	12.910	99.697
135	1.681	20.796	8.427	5.944	8.417	18.992	-0.557	19.115	12.910	100.697
150	1.681	21.504	8.427	7.860	8.417	18.992	-0.557	19.823	12.910	101.405

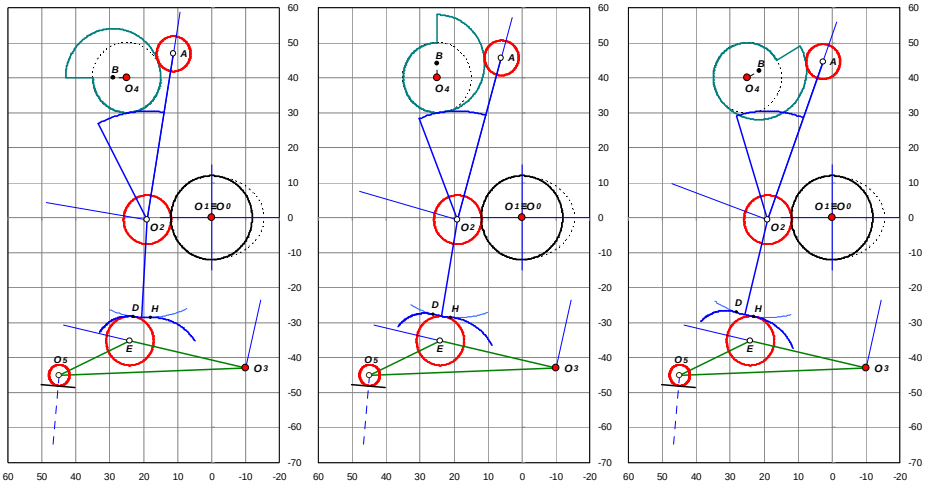

α = 0°, C_4 is identically with D | α = 90°, C_4 is between D and H | α = 150°, C_4 is identically with H

Figure 8. Mechanism's reference positions for different command angle α

In order to realize the mechanism kinematic simulation, we consider the cam is half circle half ellipse (figure 9), its equation being definite in $O_1x_1y_1$, as follows:

$$\begin{cases} x_1 = r_1^* \cos\xi \\ y_1 = -r_1 \sin\xi \end{cases}, \text{ where } r_1^* = \begin{cases} r_1, \ if \ \xi \in \left[0, \dfrac{\pi}{2}\right] \cup \left[\dfrac{3\pi}{2}, 2\pi\right] \\ 1{,}25r_1, \ if \ \xi \in \left(\dfrac{\pi}{2}, \dfrac{3\pi}{2}\right) \end{cases}.$$

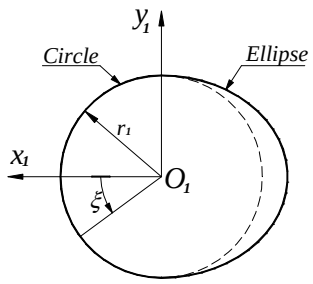

Figure 9. Semi ellipse cam design

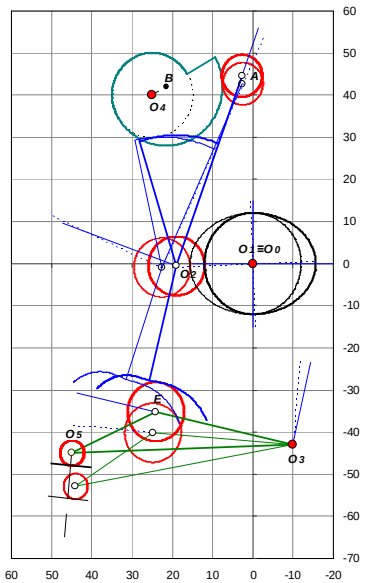

Figure 10. Mechanism kinematic overlapped positions at φ=0°, φ≈178° and α=150°

In figure 11 is designed the evolution of valve lift, for various command angle α, according to (33).

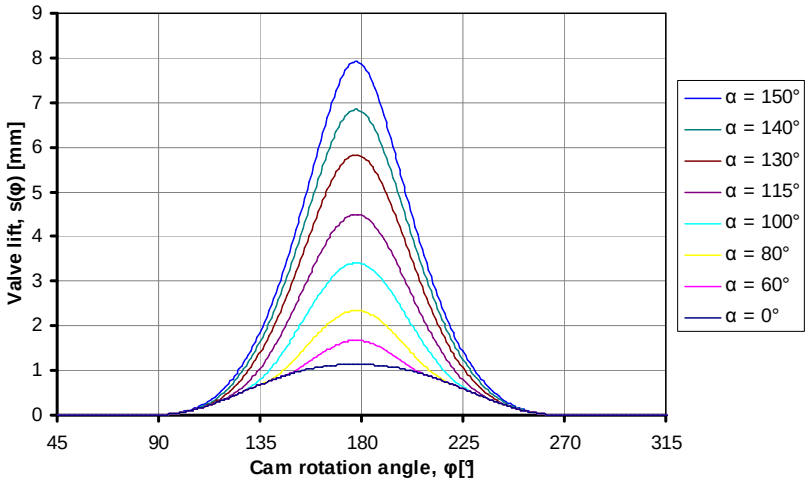

Figure 11. The evolution of valve lift for various command angle, α, generated with the semi ellipse cam

5. Conclusions

The kinematic analysis shows that the mechanism offer a continuous variation of the valve lift, with valve displacement starting from around 1 mm lift to a maximum lift around 8 mm, without changing the valve opening and closing points. The future work will be concentrated on the mechanism's synthesis and optimization.

This paper was realized with the European Program "Dezvoltarea şcolilor doctorale prin acordarea de burse tinerilor doctoranzi cu frecvenţă" POSDRU/88/1.5/S/52826.

References

[1] Artobolevski, I. *Les mécanismes dans la technique moderne*. Tome 1-5, Ed. MIR, Moskow, 1978.
[2] Artobolevski, I. *Théorie des mécanismes et des machines*, Ed. MIR, Moskow, 1977.
[3] Pandrea, N., Popa, D. *Mecanisme. Teorie şi aplicaţii CAD*, Ed. Tehnică, Bucureşti, 2000.

[4] Popa, D., Pandrea, N., Pandrea, M., Popa C.M., *Synthesis of the complex mechanisms with mobile cam*, ID: 594, 12th IFToMM World Congress, Besançon (France), June 18-21, 2007.
[5] Ronald J. Pierik, James F. Burkhard, *Design and Development of a Mechanical Variable Valve Actuation System*, SAE Technical Paper Series, 2000-01-1221.
[6] Rudolf Flierl, Daniel Gollasch, Andreas Knecht, Wilhelm Hannibal, *Improvements to a Four Cylinder Gasoline Engine Through the Fully Variable Valve Lift and Timing System UniValve*, SAE International, 2006-06P-579.
[7] ***** ATZ autotechnology, No. 5, Oct. 2009.
[8] ***** ATZ autotechnology, No. 6, Dec. 2009.
[9] ***** Automotive engineer, Apr. 2010.

Addresses:

- PhD student Stelian Mihalcea, University of Piteşti, Department of Applied Mechanics, Str. Târgul din Vale, nr.1, 110040, Piteşti, Argeş, Romania, stelian_mihalcea_07@yahoo.com